

## **Glucose Biosensor Based on Immobilization of Glucose Oxidase on Porous Screen Printed Electrodes**

*Li-Jun Bian, Lu Wang, Yin-Jian Ye, Xiao-Xia Liu\**

Department of Chemistry, Northeastern University, Shenyang, 110819

\*E-mail: [xxliu@mail.neu.edu.cn](mailto:xxliu@mail.neu.edu.cn),

*Received: 29 March 2017 / Accepted: 18 April 2017 / Published: 12 June 2017*

---

Screen printed electrodes with porous structure (PSPE) were obtained through electrochemical pretreatment. The surface morphology of PSPE exhibited a sponge-like network honeycombed by nano-size cavities. Glucose oxidase (GOD) was immobilized on the surface of PSPE by Nafion. Cyclic voltammetric results revealed that PSPE can facilitate direct electron transfer of GOD. The glucose biosensor based on GOD-PSPE showed linear amperometric responds to glucose in the ranges of 1–8 mM with high stability.

---

**Keywords:** screen printed electrode, glucose oxidase, direct electron transfer

### **1. INTRODUCTION**

Glucose is an important carbohydrate in human body, the detection of glucose is imperative for the diagnosis of diabetes mellitus. Much fascinating research and innovation have focused on effective glucose detection strategies. Glucose biosensor based on electrochemical technique and glucose oxidase (GOD) has attract much attention due to its convenience, reliability, highly sensitivity[1, 2]. The direct electron transfer (DET) between GOD and electrode is important for the development of electrochemical devices for sensing glucose. However, the DET of GOD is rarely observed on bare electrodes because the redox active center of the enzyme is shielded from the electrodes by a thick insulating protein shell[3, 4]. DET between GOD and electrode could be facilitated through chemical modification of electrodes which could provide an electron mediating function[3]. In the literatures, several material was used to modify electrode, such as carbon material, metal nanoparticle[5-8]. Porous materials with unique structure and catalytic properties have attracted considerable attention[9, 10]. Because porous materials can provide environments similar to those of redox proteins in native systems and give the protein molecules more freedom in orientation[11, 12].

Recently, screen printed electrode (SPE) have been employed for biosensors due to their low cost, flexibility in design, ease of chemical modification[13-15]. The recent study show that SPE with porous structure (PSPE) can not only offer large surface, broad potential window, low background current and high electrochemical reactivity but also can increase the detection sensitivity due to the increased surface area for electrochemical reactions. It is believed that PSPE will not only retain the attractive properties of porous electrodes but also possess the superiorities of SPE[16]. However, there is no commercial inks available for the preparation of PSPE limit its application.

In this study, we report a facile and low-cost method to produce PSPE, then GOD was immobilized on the surface of PSPE to generate a biosensor for detecting glucose. DTE was observed for the immobilized GOD, indicating that the PSPE could provide a biocompatible environment for the immobilization of the GOD. The proposed biosensor exhibits good sensitivity to glucose.

## 2. EXPERIMENTAL

### 2.1 Materials and reagents

The SPEs (working area  $0.071\text{ cm}^2$ ) were purchased from Zensor Research & Development. GOD was of biochemical purity purchased from J&K Scientific Ltd. Other chemicals were of analytical grade and used as received.

### 2.2 Preparation of PSPE and GOD modified electrode

PSPE were prepared by a two-step electrochemical method. SPE as the working electrode, a Pt plate as the counter electrode and a saturated calomel electrode (SCE) as the reference electrode. In the first step, SPE were scanned between  $-0.9$  and  $1.9\text{ V}$  at  $20\text{ mV}\cdot\text{s}^{-1}$  in a  $0.5\text{ M K}_2\text{CO}_3$  aqueous solution for ten cycles. Subsequently, the electrode were further oxidized in  $1\text{ M KNO}_3$  at  $1.8\text{ V}$  to afford PSPE. Then, the PSPE electrode were washed with deionized water to remove inorganic residuals.  $5\text{ }\mu\text{L}$  of  $6\text{ mg}\cdot\text{mL}^{-1}$  aqueous GOD solution,  $10\text{ }\mu\text{L}$  of  $0.1\text{ wt}\%$  aqueous Nafion was coated onto the PSPE surface and dried at  $4\text{ }^\circ\text{C}$ , this electrode were denoted as GOD-PSPE. When not in use, GOD-PSPE were stored in the refrigerator at  $4\text{ }^\circ\text{C}$ . For comparison, GOD was immobilized on SPE to obtain GOD-SPE at same condition.

### 2.3 Electrochemical procedures

Conductivity of SPE and PSPE were investigated using Cyclic voltammetric scans in the presence of  $5.0\text{ mM K}_3[\text{Fe}(\text{CN})_6] / \text{K}_4[\text{Fe}(\text{CN})_6]$  and  $0.1\text{ M KCl}$ . All electrochemical measurements were carried out using a three-electrode system. In  $\text{N}_2$ -saturated electrochemical test, the buffer were purged with nitrogen for at least 30 minutes, and nitrogen atmosphere was remained over the solution to protect the solution from oxygen until the test was finished. The same procedure was followed in  $\text{O}_2$ -saturated experiments except that oxygen replaced nitrogen.

### 3. RESULTS AND DISCUSSION

#### 3.1 Preparation and characterization of PSPE

Early studies showed that the surface morphology of electrode can be modified through an activation procedure. Electrochemical pretreatment is an effective procedure for improving electrode responses due to its simplicity, reproducibility, efficiency [17, 18]. The surface morphology of SPE and PSPE were shown in Fig. 1. The bare SPE surface displayed a great content of aggregated graphite nanosphere particles, whereas the PSPE surface exhibited a great number of pores. During the electrochemical treated procedure, a lot of oxygen gas evolved when the potential was higher than 1.5 V. The evolved oxygen gas could etch the surface of SPE and formed the 3D network with a large amount of channels stretching to depths [19]. Based on the observed SEM image, this porous structure expose a large surface, which was supposed to be beneficial for enhancing performance of the electrode.

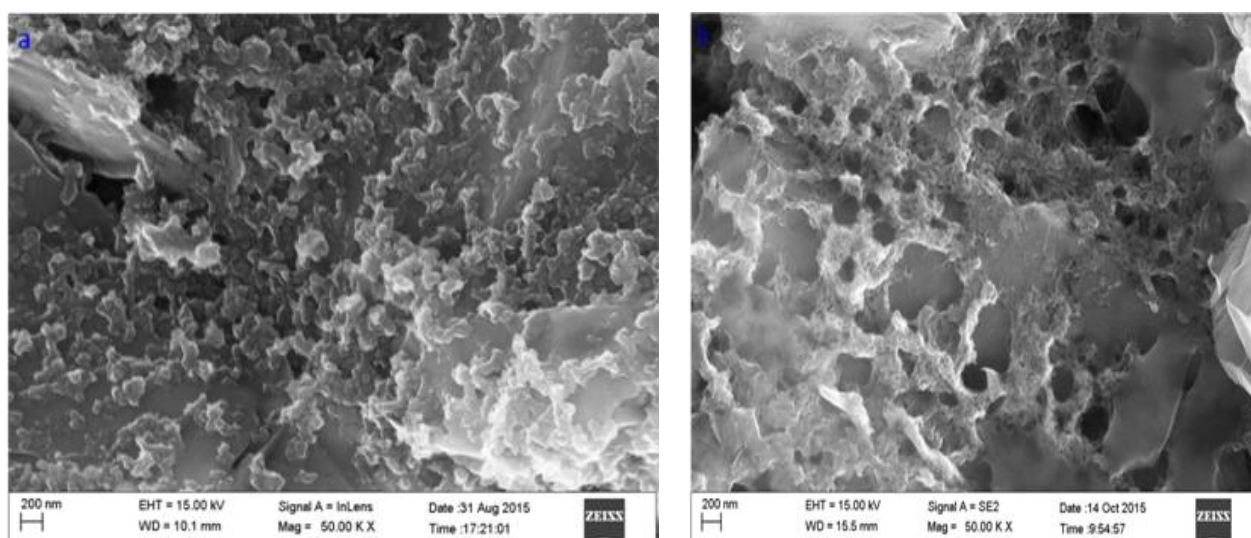


**Figure 1.** SEM image of SPE (a) and PSPE (b).

#### 3.3 Conductivity of SPE and PSPE

To investigate the electrochemical performance of SPE and PSPE, cyclic voltammetric scan was conducted in the solution containing 5 mM  $[\text{Fe}(\text{CN})_6]^{3-/4-}$  and 0.1 M KCl. An irreversible signals of  $[\text{Fe}(\text{CN})_6]^{3-/4-}$  was observed on the surface of SPE, as shown in Fig. 2. The PSPE provides a pair of quasi-reversible peaks ( $\Delta E_p$  is about 170 mV) for the electrochemical reaction of  $[\text{Fe}(\text{CN})_6]^{3-/4-}$ . The redox peak currents of the PSPE electrodes was obviously higher than that of SPE, which can be attributed to large surface area and better conductivity.

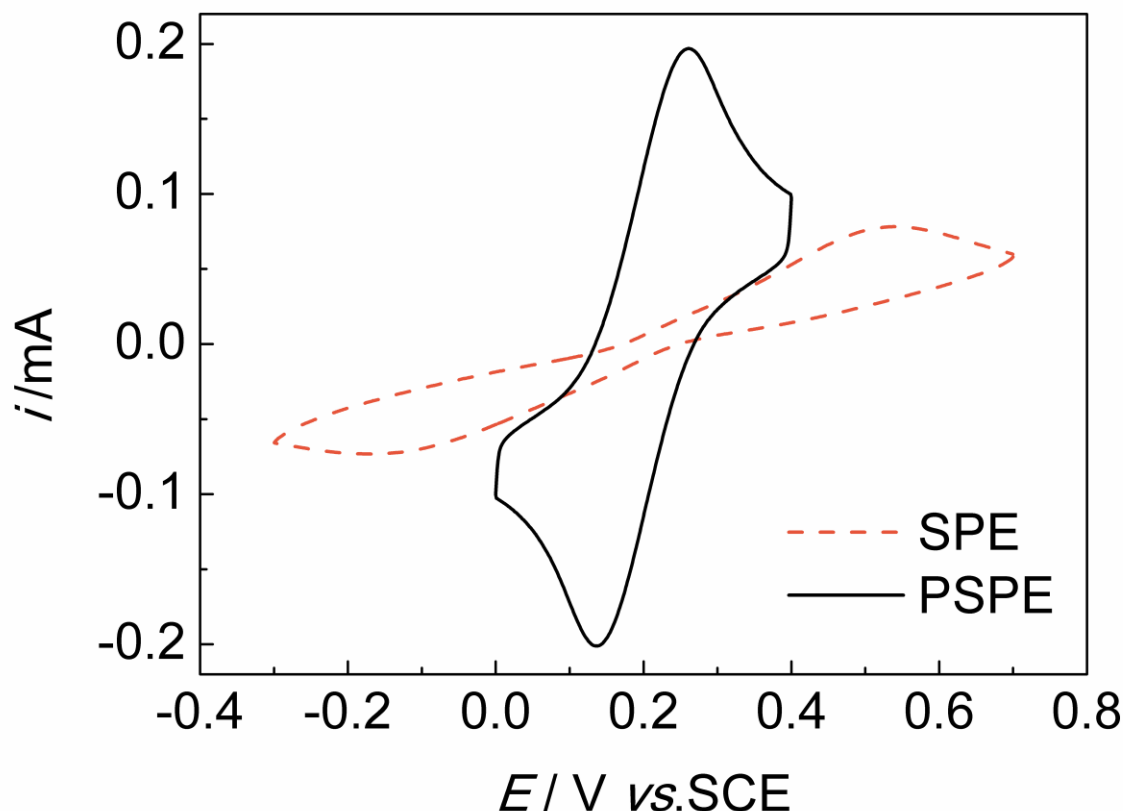


**Figure 2.** CVs of SPE and PSPE in 0.1 M, PBS pH 6.8 containing  $[\text{Fe}(\text{CN})_6]^{3-/4-}$  (10 mM, 1:1) and 0.1 M KCl at the scan rate of  $50 \text{ mV}\cdot\text{s}^{-1}$ .

### 3.4 Direct electrochemistry of GOD adsorbed on PSPE

To investigate the direct electrochemistry of GOD, cyclic voltammetric scan was conducted on the GOD-PSPE electrodes. For comparison, cyclic voltammograms (CVs) of the GOD-SPE, PSPE were obtained at the same condition. As shown in Fig.3, no redox peaks were observed for the GOD-SPE electrode (dotted line), indicating that the SPE was not a suitable medium for observing DET of GOD. PSPE did not show any peaks also, suggesting that this electrode was electro-inactive within the potential window (dashed line), the high capacitive current of PSPE was attributed to the larger surface area, this was in agreement with the result of SEM. However, a couple of well-defined and reversible redox peaks at  $-480$  and  $-505 \text{ mV}$  was observed for the immobilized GOD at the PSPE, which can be attributed to the FAD/FADH<sub>2</sub> redox couples in GOD (solid line). The peak-to-peak separation  $\Delta E_p$  ( $\Delta E_p = E_{pa} - E_{pc}$ ) is about  $25 \text{ mV}$ , indicating that the reactions of FAD/FADH<sub>2</sub> redox pairs of GOD were quasi-reversible. The direct electron transfer of GOD on PSPE could be attributed to the morphology and extraordinary electron transport property of the PSPE.

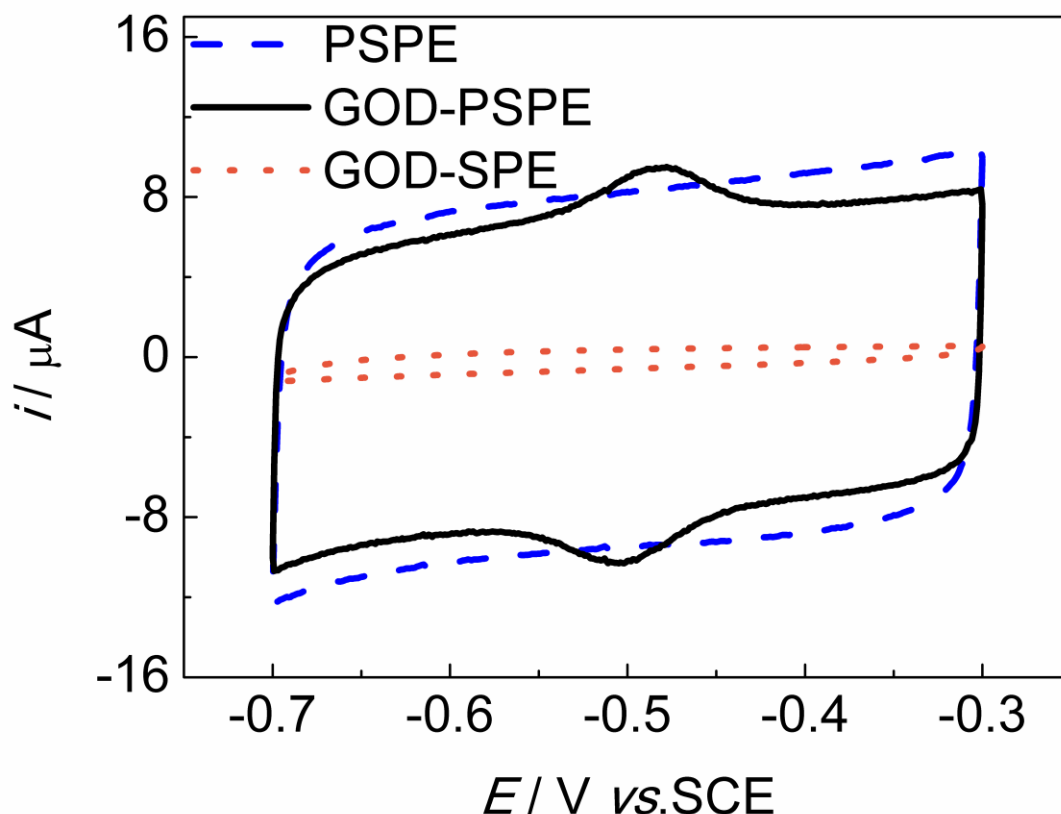


**Figure 3.** CVs of the PSPE (dashed line), the GOD-PSPE (solid line) and GOD-SPE (dotted line) in a  $N_2$ -saturated PBS solution (0.1 M, pH = 6.8) at a scan rate of  $50 \text{ mV}\cdot\text{s}^{-1}$ .

Fig.4 showed the effect of scan rate on the electrochemical response of GOD at PSPE which recorded in a  $N_2$ -phosphate buffer solution (0.1 M, pH = 6.8). The anodic peak shifted toward a more positive potential and the cathodic peak shifted toward a more negative potential slightly with increasing scan rate, possibly because of the resistance of the modified layer. The anodic and cathodic peak currents increased linearly with scan rate from 10 to  $300 \text{ mV}\cdot\text{s}^{-1}$  (inset), suggesting this was a surface-controlled process[20]. The electron transfer rate constant ( $k_s$ ) calculated using Laviron's theory, wherein the  $n\Delta E_p$  was smaller than 200 mV and  $\alpha$  was estimated to be 0.5. The obtained  $k_s$  was  $2.42 \text{ s}^{-1}$  at the scan rate of  $100 \text{ mV}\cdot\text{s}^{-1}$ , which was higher than the value observed for the GOD at 3D-KSC/NCNTs/GOD ( $2.03 \text{ s}^{-1}$ )[21], p-taurine/GOx/Nf-modified GCE( $1.38 \text{ s}^{-1}$ )[22]. The high  $k_s$  value indicated that the nano-porous structure of the PSPE provided a nano-sized environment for the intimate precursory interaction between the enzyme and the electrode, which were essential for efficient direct electron transfer.

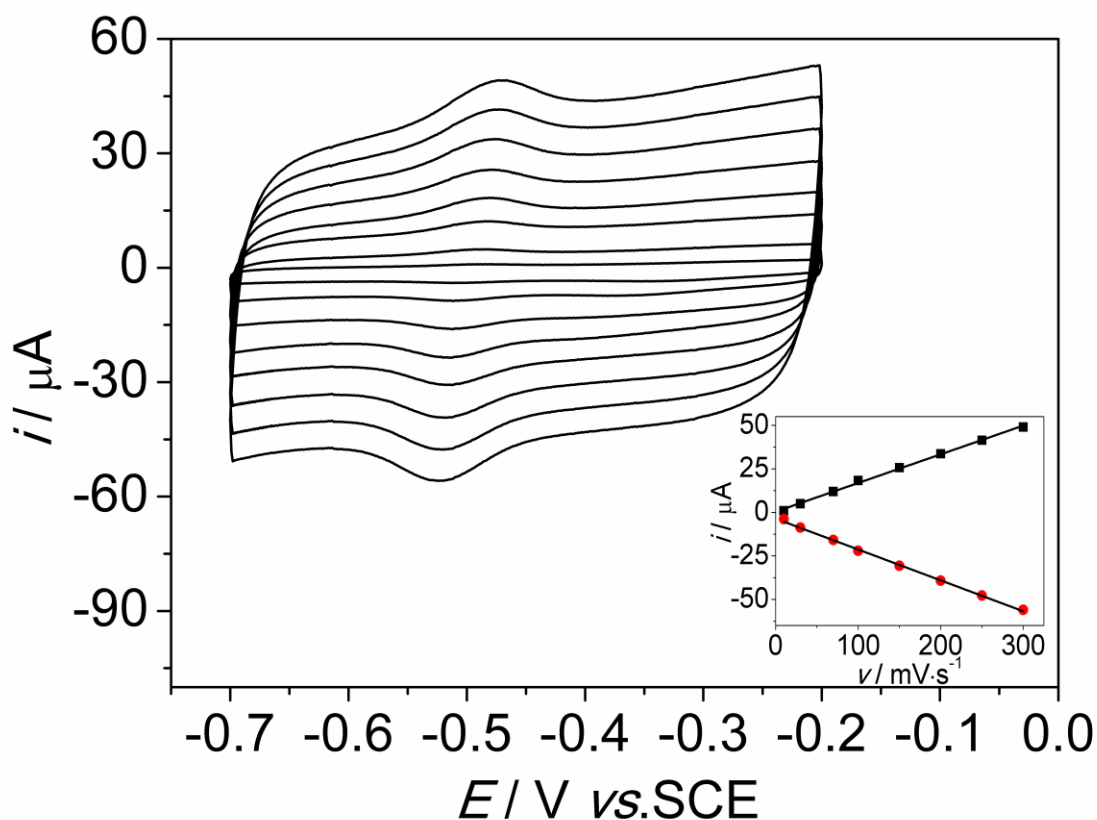


**Figure 4.** CVs of GOD-PSPE in 0.1 M  $N_2$ -saturated PBS solution at different scan rate from inner to outer: 10 to 10, 30, 70, 100, 150, 200, 250, 300  $mV \cdot s^{-1}$ .

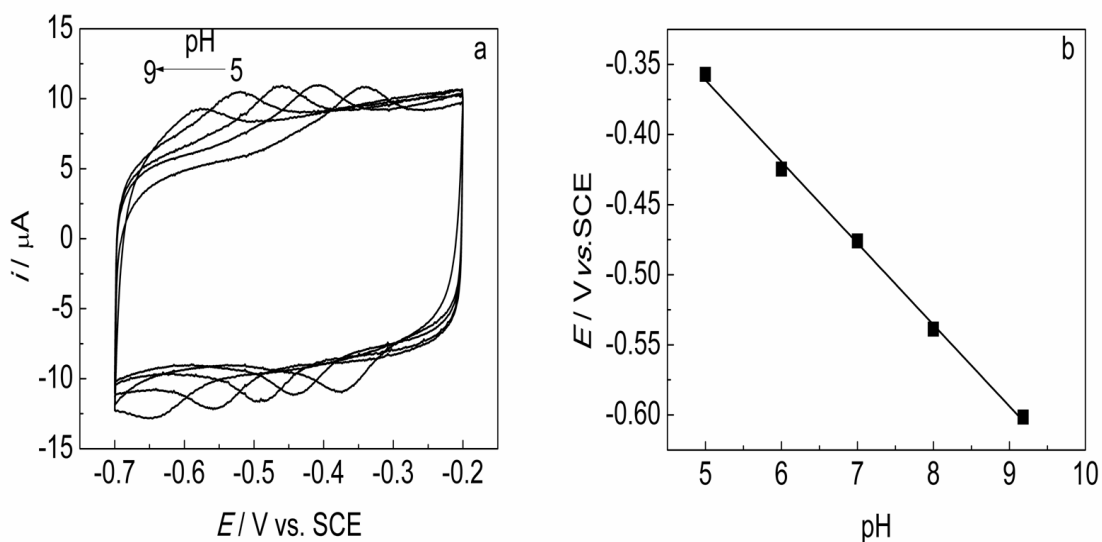
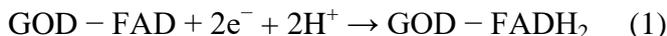


**Figure 5** (a) CVs of GOD-PSPE in 0.1 M  $N_2$ -saturated PBS solution with different pH, (b) Plot of  $E^0$  versus pH value.

The effect of pH on the direct electrochemistry of GOD was investigated by recording CVs of GOD-PSPE in  $N_2$ -saturated PBS solution with various pH=5.0 ~ 9.0 (Fig.5). A negative shift in both

the anodic and cathodic peak potentials were observed with increasing pH values, which indicated that hydrogen ion was involved in the electrode reaction of GOD. The formal potential ( $E^0 = (E_{pa} + E_{pc})/2$ ) of GOD had a linear relationship with pH from 5 to 9 with slope of  $-58.1$  mV/pH (Fig.5 inset), which was very close to the theoretical value of  $-59.0$  mV pH[23], indicating that two protons and two electrons were involved in the electron transfer process according to Eq. (1)[24].



### 3.5 Direct electrochemistry of GOD adsorbed on PSPE

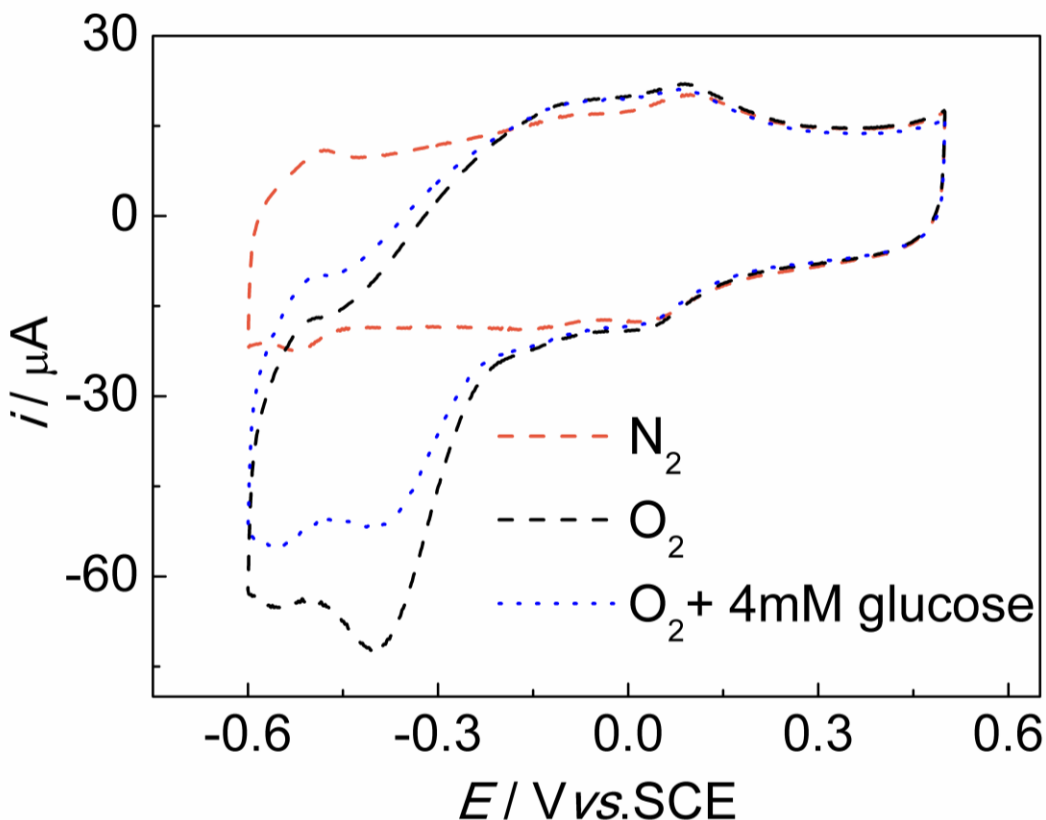
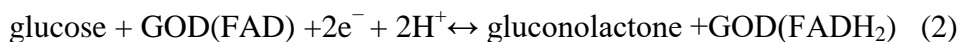


**Figure 6.** CVs of GOD-PSPE in 0.1 M  $\text{N}_2$ -saturated ,  $\text{O}_2$ -saturated PBS solution with glucose or without glucose.

To evaluate the enzymatic activity of GOD-PSPE, further electrocatalytic experiments were carried out. Fig.6 showed the CVs of the GOD-PSPE in  $\text{N}_2$  and  $\text{O}_2$  saturated PBS. A pair of well-defined redox peaks at  $-0.55$  V can be observed in both  $\text{N}_2$  and  $\text{O}_2$  saturated PBS. On the CVs of GOD-PSPE in  $\text{O}_2$  saturated PBS, an irreversible reduction peak of dissolved oxygen could be observed at around  $-0.45$  V, which indicated that PSPE had a much higher catalytic activity for oxygen reduction reaction (ORR). When glucose was added into the  $\text{O}_2$  saturated PBS, the peak current of ORR decrease (dotted line). The possible mechanism could be expressed as the following Eq. (2),(3)[25].



Since PSPE could electrocatalyze the reduction of dissolved oxygen and generate a great reduction peak current, and GOD could catalyze the oxidation process of glucose into gluconolactone accompanied by the reduction of oxygen, making it suitable for glucose determination by sensing the amount of oxygen consumed in the reduction. That is, we could detect glucose by the decrease of the cathodic peak current of ORR. Cyclic voltammetric scan was employed to investigate the electrocatalytic activity of GOD-PSPE. The CVs obtained in the presence of different concentrations of glucose in O<sub>2</sub>-saturated PBS were showed in Fig.7. Upon addition of glucose into PBS, the reduction peak current decreased. Based on the decrease of the reduction current, the resulting calibration curve was linear against the glucose concentration ranging from 1 to 8 mM ( $R^2 = 0.989$ ) (Fig. 7 inset).

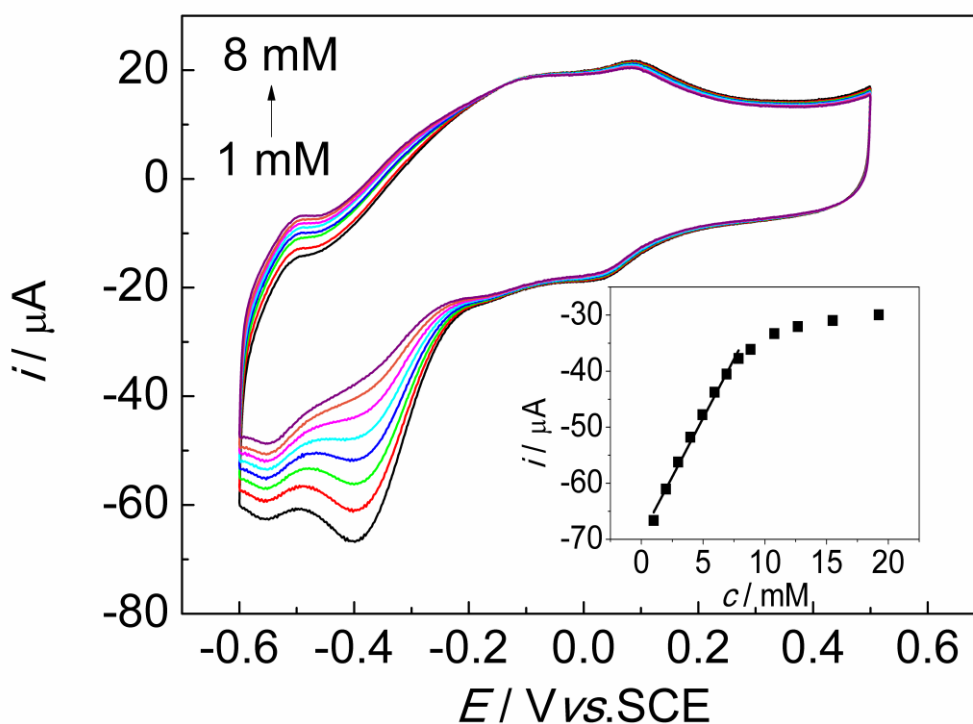


**Figure 7.** CVs of GOD-PSPE in 0.1 M O<sub>2</sub>-saturated PBS contain different concentration of glucose. Inset: Calibration curve for glucose obtained at the GOD-PSPE biosensor.

### 3.6 Stability of GOD-PSPE

The long-term stability and repeatability of the glucose biosensor are also of great importance. To check the repeatability of GOD-PSPE, the current response of one electrode toward 2 mM glucose was recorded for 8 times. The RSD (error) was 4.8%. The biosensor was stored at 4 °C in a refrigerator when not in use. The current response to 2 mM glucose ( $n = 7$ ) retained 85% after 15 days of storage. Table 1 compared the electrochemical and biosensing performance among different GOD based electrodes. It can be seen that our material is comparable with other materials. Furthermore, our

electrode can be obtained easily. These results clearly reveal that our electrode is more promising in glucose detection.

**Table 1.** Analytical parameters of glucose biosensors based on different electrodes

Biosensor composition	Mediator/signal transduction scheme	Linear range/mM	Method	Stability	Ref.
GOD-PSPE	O <sub>2</sub> reduction at -0.4 V vs.SCE	1-8	CV	15 days	This work
GOD/AuNPs/GR	PMS	0.1-10	A	1 week	[26]
GOD/PVA-Au-pphTEOS	FMCA	1-8	A	–	[27]
porous carbon/GOD/Nafion	–	0.5-9	A	2 weeks	[11]
GOD/Graphene/AuNPs/chitosan	O <sub>2</sub> reduction at -0.2 V vs.Ag AgCl	2-10	CV	–	[28]

Symbols: CV: cyclic voltammetric, AuNPs: gold nanoparticles; GR: graphite rod; PMS: N-methylphenazonium methyl sulphate; A: amperometry; PVA: polyvinyl alcohol; pphTEOS: partially prehydrolyzed tetraethyl orthosilicate; FMCA:

#### 4. CONCLUSIONS

In summary, we have developed a facile and low cost route to prepare PSPE via electrochemical pretreatment. The experimental results showed that PSPE was an attractive matrix to immobilize oxidase which can realize the DET of GOD. Due to the porous structure of PSPE, GOD-PSPE demonstrated practical linear range with satisfactory stability, repeatability for glucose detection.

#### ACKNOWLEDGEMENTS

We gratefully acknowledge financial supports from Fundamental Research Funds for the Central Universities of China (N140503002) and the National Natural Science Foundation of China (21273029).

#### References

1. H.C. Chen, Y.M. Tu, C.C. Hou, Y.C. Lin, C.H. Chen, K.H. Yang, *Anal Chim Acta*, 867 (2015) 83.
2. Y. Li, J. Han, L. Jiang, F. Li, K. Li, Y. Dong, *Analytical Letters*, 48 (2015) 1139.
3. S.-J. Bao, C.M. Li, J.-F. Zang, X.-Q. Cui, Y. Qiao, J. Guo, *Advanced Functional Materials*, 18 (2008) 591.
4. L. Xia, J. Xia, Z. Wang, *Rsc Advances*, 5 (2015) 93209.
5. X. Feng, H. Cheng, Y. Pan, H. Zheng, *Biosens Bioelectron*, 70 (2015) 411.
6. M. Wooten, S. Karra, M. Zhang, W. Gorski, *Anal Chem*, 86 (2014) 752.
7. B. Liang, X. Guo, L. Fang, Y. Hu, G. Yang, Q. Zhu, J. Wei, X. Ye, *Electrochemistry Communications*, 50 (2015) 1.

8. Y. Song, J. Chen, H. Liu, Y. Song, F. Xu, H. Tan, L. Wang, *Electrochimica Acta*, 158 (2015) 56.
9. J. Liu, X. Wang, T. Wang, D. Li, F. Xi, J. Wang, E. Wang, *ACS Appl Mater Interfaces*, 6 (2014) 19997.
10. J. Chen, R. Zhu, J. Huang, M. Zhang, H. Liu, M. Sun, L. Wang, Y. Song, *Analyst*, 140 (2015) 5578.
11. L. Jia, G. Lawrence, V.V. Balasubramanian, G. Choi, J.H. Choy, A.M. Abdullah, A. Elzatahry, K. Ariga, A. Vinu, *Chemistry*, 21 (2015) 697.
12. Z. Dai, M. Fang, J. Bao, H. Wang, T. Lu, *Analytica Chimica Acta*, 591 (2007) 195.
13. F.Y. Kong, S.X. Gu, W.W. Li, T.T. Chen, Q. Xu, W. Wang, *Biosens Bioelectron*, 56 (2014) 77.
14. T. Rungsawang, E. Punrat, J. Adkins, C. Henry, O. Chailapakul, *Electroanalysis*, 28 (2016) 462.
15. C. Karuppiah, S. Palanisamy, S.-M. Chen, V. Veeramani, P. Periakaruppan, *Microchimica Acta*, 181 (2014) 1843.
16. X. Niu, C. Chen, H. Zhao, J. Tang, Y. Li, M. Lan, *Electrochemistry Communications*, 22 (2012) 170.
17. B. Haghghi, M.A. Tabrizi, *Electrochimica Acta*, 56 (2011) 10101.
18. W.-Y. Su, S.-M. Wang, S.-H. Cheng, *Journal of Electroanalytical Chemistry*, 651 (2011) 166.
19. A. Seehuber, R. Dahint, *J Phys Chem B*, 117 (2013) 6980.
20. C.X. Guo, C.M. Li, *Phys Chem Chem Phys*, 12 (2010) 12153.
21. Y. Song, X. Lu, Y. Li, Q. Guo, S. Chen, L. Mao, H. Hou, L. Wang, *Anal Chem*, 88 (2016) 1371.
22. R. Madhu, B. Devadas, S.M. Chen, M. Rajkumar, *Anal. Methods*, 6 (2014) 9053.
23. J. Liu, Z. He, S.Y. Khoo, T.T. Tan, *Biosens Bioelectron*, 77 (2016) 942.
24. S. Palanisamy, C. Karuppiah, S.-M. Chen, *Colloids and Surfaces B: Biointerfaces*, 114 (2014) 164.
25. C. Hu, D.P. Yang, F. Zhu, F. Jiang, S. Shen, J. Zhang, *ACS Appl Mater Interfaces*, 6 (2014) 4170.